UCD CANDIDATES IN THE HYDRA CLUSTER

Elizabeth M. H. Wehner[1,2] and William E. Harris[1,3]
Accepted for publication in ApJ Letters

ABSTRACT

NGC 3311, the giant cD galaxy in the Hydra cluster (A1060), has one of the largest globular cluster systems known. We describe new Gemini GMOS (g', i') photometry of the NGC 3311 field which reveals that the *red, metal-rich* side of its globular cluster population extends smoothly upward into the mass range associated with the new class of Ultra-Compact Dwarfs (UCDs). We identify 29 UCD candidates with estimated masses $> 6 \times 10^6 M_\odot$ and discuss their characteristics. This UCD-like sequence is the most well defined one yet seen, and reinforces current ideas that the high-mass end of the globular cluster sequence merges continuously into the UCD sequence, which connects in turn to the E galaxy structural sequence.

Subject headings: galaxies: star clusters — galaxies: elliptical — galaxies: cD — galaxies: individual (NGC 3311)

1. INTRODUCTION

Ultra-Compact Dwarfs (UCDs) are a recently discovered type of old stellar system, lying between the classic globular clusters and dwarf elliptical galaxies in luminosity and scale size. Initially discovered in the Fornax cluster (Hilker 1998; Hilker et al. 1999; Drinkwater et al. 2001; Phillipps et al. 2001; Mieske et al. 2002), UCDs and UCD candidates have since been discovered in Abell 1689 (Mieske et al. 2004) and the Virgo Cluster (Haşegan et al. 2005; Jones et al. 2006; Evstigneeva et al. 2007). Transitional objects on the lower-mass end of the UCD range that connect closely with the high-mass end of the globular cluster sequence, have also been found in NGC 5128 (Rejkuba et al. 2007; Mieske et al. 2007).

Because UCDs have scale radii typically $r_{eff} \lesssim 30$ pc (not much different from extended, luminous GCs, or the nuclei of dE,Ns), they are extremely hard to find by morphology or image structure alone at galaxy distances much beyond the Virgo or Fornax clusters. Thus as yet, we know of very few UCDs. To understand what sorts of galaxy environments are most likely to produce them, we need to use a wider variety of search methods in many more locations. One such method is to employ their *photometric* similarity to the most luminous GCs and dE nuclei. If large numbers of UCDs are present in a cluster of galaxies, then they might show up as high-luminosity extensions of the normal, bimodal GC sequences that we conventionally find around giant galaxies (Harris et al. 2006; Peng et al. 2006). These candidates can then be followed up on via spectroscopy to determine their cluster memberships properties, such as metallicity, mass and age (e.g. Evstigneeva et al. 2007).

The cD galaxy NGC 3311 is the centrally dominant elliptical in the nearby Hydra cluster (Abell 1060) at d=54 Mpc ($H_0 = 73$ km/s, $\Omega_M = 0.27$, $\Omega_\Lambda = 0.73$ from NED) and is an excellent candidate for UCD-based searches of this type. The Hydra cluster ($v = 3777$ km/s) with 157 galaxy members listed by Struble et al. (1999) is perhaps twice as rich as the Fornax Cluster ($v = 1379$ km/s) in which the largest numbers of UCDs have been detected thus far. Previous photometric studies of NGC 3311 show that it contains one of the richest globular cluster (GC) systems in the local universe (Smith & Weedman 1976; Harris et al. 1983; Secker et al. 1995; McLaughlin et al. 1995; Brodie et al. 2000), making it an excellent target to search for unusually massive clusters and stripped dE nuclei.

As part of a new imaging program to investigate globular cluster systems (GCSs) around cD galaxies, we obtained deep (g', i') photometry of NGC 3311 to investigate the nature of the new "mass/metallicity relation" recently discovered to affect the metal-poor GC sequence (Harris et al. 2006; Strader et al. 2006; Mieske et al. 2006). Our results have revealed an extension of the red, metal-rich branch of the globular cluster system up to unusually high luminosities ($-10 > M_{g'} > -12$), into the UCD regime. In § 2 we present our observations and data reduction. In § 3 we examine the radial distributions and masses of our candidate UCDs, and we discuss the implications of our results in § 4.

2. OBSERVATIONS AND REDUCTIONS

We obtained deep (g', i') images of NGC 3311 using the GMOS imager on Gemini South, which has a $5.5' \times 5.5'$ field of view (FOV) and a scale of $0.146''/pix$ after 2×2 binning. Data were taken on the nights of February 8 and March 23, 2006, under dark, photometric conditions, with an average seeing of $0.5''$. The total integration time in each of (g', i') was 3900s. The data were reduced with the GEMINI package in IRAF[4], calibrated with Landolt standard stars (Landolt 1992), and transformed to (g', i') with the equations of Fukugita et al. (1996)[5]. For the

---

[1] Department of Physics & Astronomy, McMaster University, Hamilton, ON L8S 4M1, Canada
[2] wehnere@physics.mcmaster.ca
[3] harris@physics.mcmaster.ca

[4] IRAF is distributed by the National Optical Astronomy Observatories, which are operated by the Association of Universities for Research in Astronomy, Inc., under cooperative agreement with the National Science Foundation.

[5] A complete set of the Landolt (1992) standard stars transformed from the Johnson-Cousins system into the Sloan filter set has been compiled by the authors and is available online at http://www.elizabethwehner.com/astro/sloan.html
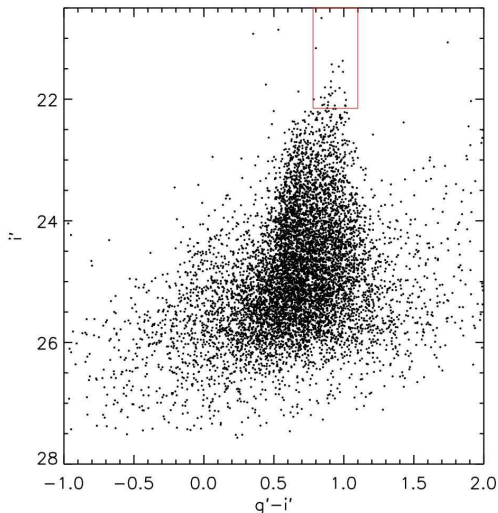
FIG. 1.— Color-magnitude Diagram for the globular clusters around NGC 3311. Note that the color index plotted here is the *dereddened* value $(g' - i')_0$. The box (outlined in red in the online version) indicates the location in color-magnitude space of the UCD candidates.

FIG. 2.— i'-band GMOS field of NGC 3311 (center) and NGC 3309 (upper right). Locations of UCD candidates are marked by circles. The field size shown is $5.5'$ across. The shadow of the guide probe is seen at the bottom. North is up, and East is to the left.

photometric calibration, we used standard stars (with a very limited range in airmass) to measure a zero point for single (g', i') exposures taken at the same airmass as our NGC 3311 images. The small amount of fringing in i' was successfully removed with a calibration fringe frame from the Gemini archives. Our photometry reached limiting magnitudes (50% detection completeness) of $g'(lim) = 26.7$ and $i'(lim) = 26.2$, deep enough to reach near the GC luminosity function turnover point.

3. PHOTOMETRIC RESULTS

Once the final image and calibration were obtained, we used the stand-alone version of DAOPHOT (daophot4) to obtain photometric measurements in g' and i' of each object in our $5.5'$ FOV. In total, we detected 8108 star-like objects, the vast majority of which clearly belong to the globular cluster population. The color-magnitude diagram (CMD) is shown in Figure 1.[6]

The CMD shows the GC population in the expected color range $0.4 \lesssim g' - i' \lesssim 1.2$ as well as field contamination at faint levels on both the redder and bluer sides. Although this CMD is interesting in several ways (to be discussed in our upcoming Paper II), perhaps the most unusual feature can be found at the brightest magnitudes where we note the presence of an extension up to very high luminosities on the red (metal-richer) side of the GC population. This distribution is unlike any we have seen before in other giant E galaxies (e.g. Harris et al. 2006). We find 29 objects brighter than $i' \leq 22.15$, the point where the blue side of the GC distribution reaches its top end. Intriguingly, it is only the red branch of the GC population that extends toward still higher luminosities. At $M_{i'} \lesssim -11.7$, these are very luminous GCs. Few such objects appear even in the composite sample of many thousands of GCs in eight cD galaxies studied

by Harris et al. (2006), and easily reach up to the range occupied by UCDs and dE nuclei. Because of their connection with the red GC sequence, these UCD candidates could also be categorized as dwarf-globular transition objects (DGTOs), a term coined by Haşegan et al. (2005) to indicate the difficulty in truly distinguishing compact dwarfs from massive globular clusters.

How many of these objects are real? One concern may be blending, i.e. two ordinary globular clusters aligned along the line of sight, boosting the observed magnitude up to ~ 0.75 magnitudes. However, using the equation for the number of expected blends on a frame from Harris et al. (2007), we find that for GCs brighter than $i' \simeq 23$, we expect only 0.47 blends across our entire frame. If instead these objects were foreground stars, we would expect them to be more evenly distributed in color and randomly distributed across the frame (as we show is not the case in Figures 2 and 3).

We also note that four objects fall blueward of the clear sequence seen in Fig. 1. Although perhaps not part of this sequence, these may be UCDs as well, and so we include them. One of these objects (number 13 in Table 1) falls near the top of the blue sequence, although we cannot determine if this is actually a member/extension of the blue sequence, or merely a coincidental overlap. The remaining objects, those in the red sequence, extend up to $M_{i'} = -12.4$ ($i' = 21.4$).

One of our first goals is to establish whether or not these objects are associated with NGC 3311. Figure 2 shows the location of each UCD candidate. Close visual inspection of each object reveals them to be (apparently) stellar in nature, not obviously background galaxies. Furthermore, since they appear to be distributed across the field of view rather than clumped, we can rule out contamination from a distant background galaxy cluster.

But how do these objects relate to NGC 3311? Figure 3 shows the cumulative radial distribution for the UCD candidates, relative to the center of NGC 3311, as well as the cumulative distribution for the GC population as

---

[6] Our FOV contains the Hydra gE NGC 3309, which has been found to contribute $\lesssim 10\%$ of the GC population in the field (McLaughlin et al. 1995; Brodie et al. 2000). Nevertheless, we exclude only those objects in the inner $r = 120$ pixels around the centers of both giant galaxies.
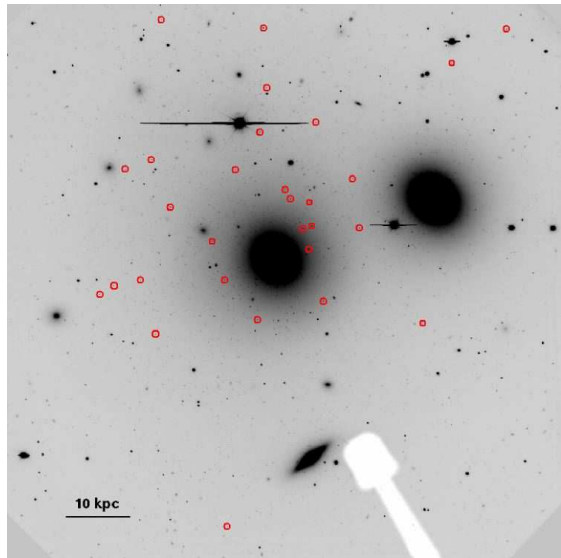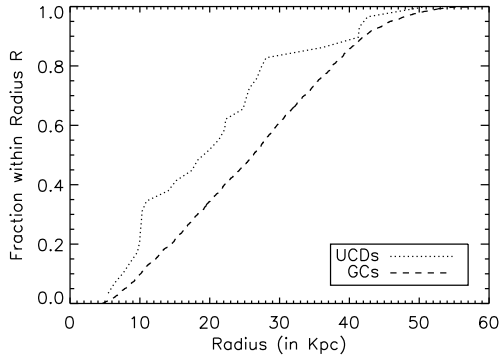
FIG. 3.— Radial distribution of UCD candidates (dotted line) and globular clusters (dashed line) relative to the center of NGC 3311. The distributions are plotted in cumulative form, as the fraction of the total population lying within projected radius R.

a whole. (In order to plot the GCS radial distribution, we used only globular clusters on the side of the field opposite to NGC 3309.) A Kolmogorov-Smirnov two-sample test on these two radial distributions shows them to be different at more than 99 percent confidence. The difference is in the sense (see Figure 3) that the UCDs are *at least* as centrally concentrated as the GCs; in other words, they are more likely to be connected with the GCS rather than the more extended Hydra potential well as a whole.

Next we estimate the mass of each UCD candidate (hereafter UCDs), for which the choice of M/L is critical. While globular clusters typically have $(M/L)_V \sim 1 - 3$, UCDs have M/L as high as 6-9 $M_\odot/L_\odot$ (Haşegan et al. 2005; Evstigneeva et al. 2007), although simulations by Fellhauer & Kroupa (2006) suggest that tidal interactions with the centers of their host galaxies *may* disturb a UCD from its virial equilibrium, thereby leading to an overestimation of its M/L ratio. Hilker et al. (2007) found that 5 UCDs in Fornax ranged from 3-5 $M_\odot/L_\odot$, exactly the same $(M/L)_V$ range found for Virgo UCDs (Evstigneeva et al. 2007). If we assume, rather, that our objects are more similar to high-mass globular clusters, then we can look to simple stellar population models for predicted M/L ratios. Bruzual & Charlot (2003) models for old stellar populations ($t \sim 12$ Gyr) indicate that $(M/L)_V$ can range from 1-6 $M_\odot/L_\odot$, increasing systematically with metallicity. The red peak of the GCS falls near $(V-I)_0 \sim 1.1$, or $[Fe/H] \sim -0.5$, which in the Bruzual & Charlot models corresponds to $M/L \sim 2$. The average M/L ratio in Rejkuba et al. (2007)'s newly discovered relationship between M/L and mass for UCDs is ~ 3. Since this most closely represents the undefined nature of our objects, and is a midpoint between the aforementioned low ($M/L \sim 1$) and high ($M/L \sim 5$) ends, we adopt a compromise $(M/L)_V = 3$ for our UCD candidates.

We used the g' magnitudes to calculate a total luminosity for each UCD in our sample. The solar luminosity $M_{g'\odot} = 5.06$ was adopted from Yasuda et al. (2001). The g'-band was chosen over the i'-band for calculating masses in order to most closely match the expected M/L ratio, which is well documented for both the Johnson B and V bands but not so extensively in either the infrared or the Sloan filter system. In order to calculate absolute magnitudes, we adopted a distance modulus of

$(m-M)_0 = 33.68$ and a reddening of $E_{(g'-i')} = 0.158$ (from NED). The raw i' magnitudes, the $(g'-i')_0$ dereddened colors, and the estimated masses for each object are listed in Table 1, along with the V and $V-I$ data from HST/WFPC2 if available, and the coordinates and the projected distance of each object from the center of NGC 3311. From the foregoing discussion, we emphasize that these calculated masses should be viewed only as plausible estimates and might be, if anything, lower limits.

4. DISCUSSION

The masses of these high-end GCs are all above $6 \times 10^6 M_\odot$ and extend to almost $3 \times 10^7 M_\odot$. From their radial distribution, they are clearly within the Hydra cluster (and possibly specifically associated with its cD galaxy, NGC 3311). Structurally, they are very compact: A normal dwarf-galaxy scale length of 300 pc (Deady et al. 2002) would give $FWHM \sim 2''$ on our GMOS images, whereas our "superluminous GCs" are completely unresolved at the 0.5'' resolution of our GMOS images, implying that their scale radii are $r_{eff} \lesssim 50$ pc. A better limit on their scale sizes would, however, come from HST imaging with its 0''.1 resolution. Ten of our UCD candidates fall within the WFPC2 field near NGC 3311 studied by Brodie et al. (2000) and two additional UCD candidates fall on the WFPC2 archival data for NGC 3309. We extracted these images from the HST Archive and measured them. We find that the 12 candidates, all on the undersampled WF frames, have FWHMs ranging from 0''.204 to 0''.250, averaging 0''.222 ± 0''.006. By comparison, the unresolved PSF on WF2,3,4 has a measured $\langle FWHM \rangle = 0''.208 \pm 0''.004$. The UCD candidates are therefore *marginally* resolved (at the $2-\sigma$ level). Subtracting $FWHM_{UCD}$ in quadrature from $FWHM_{PSF}$, we can then estimate *very roughly* that our candidates have scale sizes equivalent to an effective diameter of $\simeq 20$ pc. This is only a crude estimate but is precisely in the r_{eff} range occupied by the known Fornax UCDs, most of the Virgo UCDs, and the DGTOs (Evstigneeva et al. 2007; Haşegan et al. 2005). In Table 1, we list the V and $(V-I)$ measurements of the 12 overlapping candidates as obtained from the WFPC2 data. They average $\langle V - I \rangle_0 = 1.1$, entirely similar to normal red-sequence GCs.

There are now three main scenarios to explain UCDs. One possibility is that UCDs are the nuclei of dE,N galaxies that have been stripped of their envelopes via galaxy "threshing," on multiple passes through a larger galaxy (Bekki et al. 2001). Fellhauer & Kroupa (2002) suggest that UCDs may also form from the agglomeration of young massive star clusters in locations of ongoing, violent star formation. A third possibility is that UCDs are simply high-mass extensions of globular clusters and share a common formation mechanism with their lower mass counterparts. Evidence can be found for each of these formation scenarios (e.g. Haşegan et al. 2005), suggesting that UCDs may not be a homogenous population; rather, objects can end up as UCDs in different ways.

Rejkuba et al. (2007) and Barmby et al. (2007) provide strong new evidence from M/L ratios and structural sizes of the most massive known GCs in NGC 5128 and M31 that they may form the beginning of the long-missing bridge between the GC and dwarf-E sequence.

It has long been thought that GCs had a constant scale size $r_h \sim 3$ pc independent of mass, whereas $r_h \sim M^{0.6}$ for E galaxies (e.g. Haşegan et al. 2005; Barmby et al. 2007). This new evidence suggests that massive star clusters ($10^7 M_\odot$ and above) must somehow form at increasingly larger scale size regardless of their environment. Recent work by Evstigneeva et al. (2007) on the Fornax and Virgo UCDs in the range of $10^7 - 10^8 M_\odot$ further traces out a continuous sequence between globular clusters, UCDs, dE nuclei and de,Ns, and giant ellipticals in velocity dispersion and magnitude space. A clear sequence also exists in the $\kappa_1 - \kappa_3$ plane of κ-space, a fundamental plane for dynamically hot systems originally defined by Bender et al. (1992).

The UCD candidates in NGC 3311 mark out the clearest connection of such objects with GCs yet found within any one galaxy. This result is consistent with the idea that there may be a smooth bridge in structural parameters between these and the high-mass UCDs. Indeed, given that evidence has been presented to support a) the idea that UCDs can form via diverse mechanisms, rather than a single, evolutionary path (e.g. Haşegan et al. 2005; Evstigneeva et al. 2007), and b) the existence of a continuous sequence between these objects in structural parameter space, it seems that regardless of how a compact stellar system is assembled, it will strongly converge to a structure that falls within this unified sequence. The sequence in NGC 3311 provides an excellent opportunity to further trace this "bridge" of intermediate-mass old stellar systems. A logical next step would be radial velocity measurements, which would help decide whether they belong more to NGC 3311 (and thus formed along with its GCs) or to the general Hydra cluster.

REFERENCES

Barmby, P. G., McLaughlin, D. E., Harris, W. E., Harris, G. L. H., & Forbes, D. A. 2007, AJ, 133, 2764

Bekki, K., Couch, W. J., & Drinkwater, M. J. 2001, ApJ, 552, L105

Bender, R., Burstein, D., & Faber, S. M. 1992, ApJ, 399, 462

Brodie, J. P., Larsen, S. S., & Kissler-Patig, M. 2000, ApJ, 543, L19

Bruzual, G., & Charlot, S. 2003, MNRAS, 344, 1000

Deady, J. H., Boyce, P. J., Phillipps, S., Drinkwater, M. J., Karick, A., Jones, J. B., Gregg, M. D., & Smith, R. M 2002, MNRAS, 336, 851

Drinkwater, M. J., et al. 2000, A&A, 355, 900

Evstigneeva, E. A., Gregg, M. D., Drinkwater, M. J., & Hilker, M. 2007, AJ, 133, 1722

Fellhauer, M. & Kroupa, P. 2002, MNRAS, 360, 642

Fellhauer, M. & Kroupa, P. 2006, MNRAS, 367, 1577

Fukugita, M., Ichikawa, T., Gunn, J. E., Shmiasaku, K., & Schneider, D. P. 1996, AJ, 111, 1748

Harris, W. E., Smith, M. G., & Myra, E. S. 1983, ApJ, 272, 456

Harris, W. E., Whitmore, B. C., Karakla, D., Okon, W, Baum, W. A., Hanes, D. A., & Kavelaars, J. J. 2006, ApJ, 636, 90

Harris, W. E., Harris, G. L. H., Layden, A. C., & Stetson, P. B. 2007, AJ, 134, 43

Haşegan, M. et al. 2005, ApJ, 627, 203

Hilker, M., Infante, L., & Richtler, T. 1999, A&A, 138, 55

Hilker, M. 1998, PhD thesis, Univ. Bonn

Hilker, M., Baumgardt, H., Infante, L., Evstigneeva, E., & Gregg, M. 2007, å, 463, 119

Jones, J. B., et al. 2006, AJ, 131, 312

Landolt, A. U. 1992, AJ, 104, 340

McLaughlin, D. E., Secker, J., Harris, W. E., & Geisler, D. 1995, AJ, 109, 1033

Mieske, S., Hilker, M., & Infante, L. 2002, A&A, 383, 823

Mieske, S., et al. 2004, AJ, 128, 1529

Mieske, S. et al. 2006, ApJ, 653, 193

Mieske, S., Hilker, M., Jordan, A., Infante, L., & Kissler-Patig, M. 2007, astro-ph/0706.2724v1

Peng, E. W., et al. 2006 ApJ, 639, 95

Phillipps, S., Drinkwater, M. J., Gregg, M. D., & Jones, J. B. 2001, ApJ, 560, 201

Rejkuba, M., Dubath, P., Minniti, D., & Meylan, G. 2007, astro-ph/0703385

Secker, J., Geisler, D., McLaughlin, D. E., & Harris, W. E. 1995, AJ, 109, 1019

Smith, M. G. & Weedman, D. W. 1976, ApJ, 205, 709

Strader, J., Brodie, J. P., Spitler, L, & Beasley, M. A. 2006, AJ, 132, 2333

Struble et al. 1999, ApJS, 125, 35

Yasuda, N., et al. 2001, AJ, 122, 1104

TABLE 1

UCD	$M_{g'}$	Mass $(10^6 M_\odot)$	i'	$(g' - i')_0$	V	$V - I$	RA	Dec	D (Kpc)
1	-12.3	27.1	20.67	0.84	-	-	10:36:43.320	-27:29:24.19	36.1
2	-11.9	17.9	21.16	0.80	-	-	10:36:32.456	-27:29:24.88	51.0
3	-11.5	12.4	21.37	0.99	-	-	10:36:41.160	-27:31:21.90	7.6
4	-11.5	12.6	21.43	0.91	22.24	1.15	10:36:47.481	-27:31:10.59	18.3
5	-11.4	11.7	21.46	0.96	-	-	10:36:44.923	-27:34:20.21	42.6
6	-11.3	10.5	21.55	0.99	22.54	1.28	10:36:40.639	-27:32:06.42	10.1
7	-11.4	11.2	21.55	0.92	-	-	10:36:50.016	-27:31:57.35	25.7
8	-11.2	9.8	21.71	0.91	-	-	10:36:34.899	-27:29:44.90	41.3
9	-11.1	8.9	21.81	0.91	-	-	10:36:43.487	-27:30:26.04	19.9
10	-11.0	9.2	21.81	0.87	-	-	10:36:49.500	-27:30:48.07	27.3
11	-11.1	8.3	21.82	0.97	-	-	10:36:42.354	-27:31:00.00	10.9
12	-11.0	8.2	21.87	0.94	-	-	10:36:41.249	-27:31:07.80	10.3
13	-11.3	10.4	21.87	0.68	-	-	10:36:43.186	-27:29:59.72	26.8
14	-10.9	7.5	21.89	1.01	22.84	1.27	10:36:43.578	-27:32:17.43	10.0
15	-11.0	8.1	21.90	0.92	22.81	1.18	10:36:48.133	-27:32:26.02	22.1
16	-11.0	8.2	21.92	0.89	23.03	1.22	10:36:36.203	-27:32:19.59	25.2
17	-11.0	7.9	21.94	0.91	-	-	10:36:40.978	-27:30:20.10	22.3
18	-11.0	8.2	21.97	0.84	-	-	10:36:41.290	-27:31:35.55	5.5
19	-11.0	8.0	21.98	0.86	22.65	1.07	10:36:48.321	-27:30:42.38	24.8
20	-11.1	8.3	22.00	0.79	22.78	1.12	10:36:45.606	-27:31:30.90	10.2
21	-10.8	6.7	22.01	1.02	-	-	10:36:42.100	-27:31:05.70	9.6
22	-10.9	7.3	22.05	0.89	22.96	1.22	10:36:45.055	-27:31:53.86	8.6
23	-10.9	7.2	22.09	0.86	23.05	1.23	10:36:50.646	-27:32:02.50	28.1
24	-10.8	6.9	22.10	0.89	-	-	10:36:47.876	-27:29:19.14	41.4
25	-10.9	7.2	22.10	0.85	-	-	10:36:41.556	-27:31:23.32	6.4
26	-10.7	6.2	22.10	1.01	-	-	10:36:39.316	-27:30:53.73	17.4
27	-10.8	6.6	22.10	0.94	23.04	1.16	10:36:44.577	-27:30:48.51	15.2
28	-10.7	6.2	22.11	1.01	23.24	1.33	10:36:39.024	-27:31:22.96	14.0
29	-10.8	6.7	22.15	0.88	23.05	1.16	10:36:48.803	-27:31:53.72	21.3